Inorganic Chemistry

pubs.acs.org/IC Article

A Combined Spectroscopic and Protein Crystallography Study Reveals Protein Interactions of Rh^{I}(NHC) Complexes at the Molecular Level

Isabelle M. Daubit,[#] Matthew P. Sullivan,[#] Milena John, David C. Goldstone, Christian G. Hartinger, and Nils Metzler-Nolte*

Cite This: https://dx.doi.org/10.1021/acs.inorgchem.0c02438 Read Online

ACCESS | Metrics & More | Article Recommendations | Supporting Information

ABSTRACT: While most Rh−N-heterocyclic carbene (NHC) complexes currently investigated in anticancer research contain a Rh(III) metal center, an increasing amount of research is focusing on the cytotoxic activity and mode of action of square-planar [RhCl(COD)(NHC)] (where COD = 1,5-cyclooctadiene) which contains a Rh(I) center. The enzyme thioredoxin reductase (TrxR) and the protein albumin have been proposed as potential targets, but the molecular processes taking place upon protein interaction remain elusive. Herein, we report the preparation of peptide-conjugated and its nonconjugated parent [RhCl(COD)(NHC)] complexes, an in-depth investigation of both their stability in solution, and a crystallographic study of protein interaction. The organorhodium compounds showed a rapid loss of the COD ligand and slow loss of the NHC ligand in aqueous solution. These ligand exchange reactions were reflected in studies on the interaction with hen egg white lysozyme (HEWL) as a model protein in single-crystal X-ray crystallographic investigations. Upon treatment of HEWL with an amino acid functionalized [RhCl(COD)-(NHC)] complex, two distinct rhodium adducts were found initially after 7 d of incubation at His15 and after 4 weeks also at Lys33. In both cases, the COD and chlorido ligands had been substituted with aqua and/or hydroxido ligands. While the histidine (His) adduct also indicated a loss of the NHC ligand, the lysine (Lys) adduct retained the NHC core derived from the amino acid L-histidine. In either case, an octahedral coordination environment of the metal center indicates oxidation to Rh(III). This investigation gives the first insight on the interaction of Rh(I)(NHC) complexes and proteins at the molecular level.

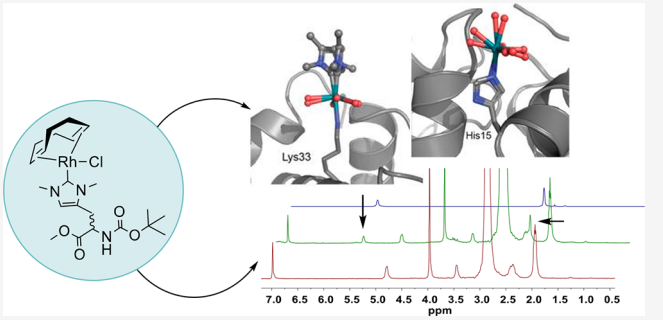

INTRODUCTION

Soon after the discovery of cisplatin, which contains a Pt(II) center, Giraldi et al. investigated Rh(I) complexes which were structurally and electronically similar to cisplatin and determined their anticancer activities.[1,2] Some of the investigated compounds were able to cure mice bearing Ehrlich ascites sarcoma,[1,2] however research in the area quickly ceased. More recently, Rh complexes investigated for their anticancer properties contain a metal center in the oxidation state +III,[3−9] while complexes of Rh(I) are rather investigated for their catalytic activities.[10−12] Among the few examples of Rh(I) complexes investigated in the field of anticancer research, those of the overall formula [RhX(COD)(NHC)] (where COD = 1,5-cyclooctadiene, NHC = N-heterocyclic carbene, and X = halide) represent the majority. Their most valuable feature is represented by the NHC ligand which can be functionalized to suit the desired application either at the imidazolium backbone or at one or both of the nitrogen atoms. This provides not only a scaffold for a broad variety of structures but also a handle to control the stability of the complex.[13−16] The possibility to include an imidazolium moiety in virtually every possible structure is most impressively illustrated by peptide conjugated examples of [RhCl(COD)-(NHC)] complexes reported in the literature, where the NHC ligand represents a methylated histidine (His) derivative that was either directly used for complexation[17] or embedded in a peptide scaffold, thus forming a peptide NHC ligand.[18,19]

The *in vitro* investigation of the cytotoxic activity of [RhCl(COD)(NHC)] complexes revealed IC_{50} values in the high nanomolar to low micromolar range.[20−28] This effect was correlated to the structure of the NHC ligand driving the cellular uptake of the respective complex[21,28] and the respective cancer cell line under investigation. Initial work on the *in vivo* activity of a [RhCl(COD)(NHC)] complex in a

Received: August 14, 2020

Scheme 1. Synthesis of Imidazolium Functionalized His Derivatives 5 and 6 and SPPS of Imidazolium Functionalized Peptide 7

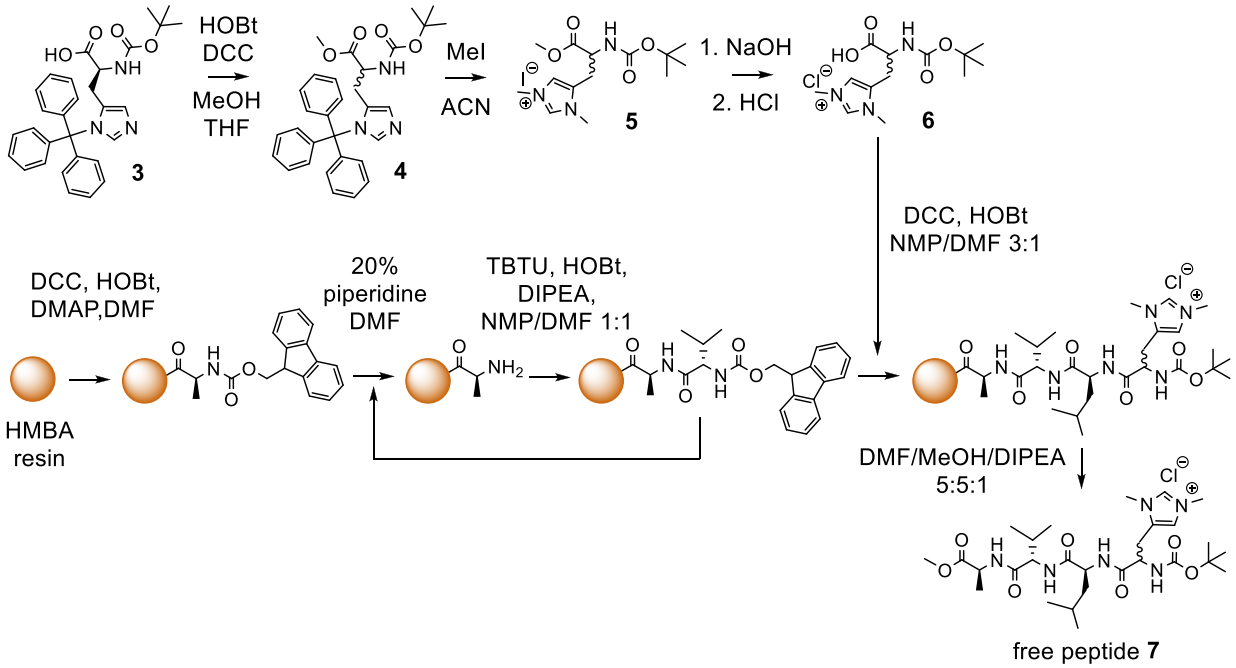

HepG2 xenograft model in nude mice showed the ability to reduce tumor weight of mice treated with 10 mg/kg of the complex by up to 45%.[28] However, the mode of action of the complexes is still under debate. While several reports about the interaction of the complexes with free deoxyribonucleic acid (DNA) exist,[20,22] the amount of nuclear rhodium content after treatment of cells with a respective complex has not been higher than 1−2%, casting doubt on DNA as their main cellular interaction site.[22] Instead, it has been proposed that DNA damage represents a secondary effect, caused by the generation of reactive oxygen species inside of the cancer cells after treatment with [RhCl(COD)(NHC)] complexes that finally leads to cell cycle arrest.[24] This hypothesis is in agreement with reports describing the ability of the complexes to act as cell cycle inhibitors.[20,23,28] Besides binding to DNA, interactions with proteins including albumin[22] and thioredoxin reductase (TrxR) have been described.[24,28] However, the molecular nature of the interaction of the complexes with DNA or proteins remains poorly investigated.

Hydrolytic stability studies of [RhCl(COD)(NHC)] complexes revealed a potential to form aqua or hydroxido complexes by exchange of the chlorido ligand.[23] Additionally, loss of the NHC ligand in aqueous solution eventually led to the formation of dimeric chlorido-bridged structures.[23] An investigation of their ability to interact with 9-ethylguanine, a DNA model base, showed that the chlorido ligand was readily exchanged by the N_7 of the nucleobase.[25] While the molecular nature of [RhCl(COD)(NHC)]−protein interactions has not been investigated so far, the binding of structurally related [IrCl(COD)(NHC)] complexes to cytochrome C and lysozyme has been reported to proceed through loss of the COD and chlorido ligands along with an oxidation of the metal center from +I to +III.[29−32] Further in depth investigation of this process led to the conclusion that formation of a solvent surrounded iridium-NHC intermediate is the initial step of this interaction.[33] Adducts of the general type M(NHC) with proteins were characterized by Merlino et al. for Au(NHC) complexes and the model protein thaumatin.[34] Hen egg white lysozyme (HEWL, containing 129 amino acids) is another model protein that has been widely used for metal−protein interaction studies due to its small molecular weight of 14.3 kDa.[30,35−43] For example, the interaction of the M(NHC) complex [dichlorido(η^6-p-cymene)(1,3-dimethylbenzimidazol-2-ylidene)ruthenium(II)] and HEWL revealed that the chlorido ligand was exchanged with the imidazole of His15 of the protein. This interaction was concomitant to the loss of *p*-cymene and coordination of arginine (Arg)14.[44,45] Over a longer period of time, a secondary interaction with lysine (Lys)33 of HEWL was found.[46] Lys33 has been suggested as a potential site for interaction with platinum complexes.[47,48]

In order to add to the understanding of the behavior of M(NHC) complexes in biological environments, we herein report investigations on the hydrolytic stability of a [RhCl(COD)(NHC)] complex and a peptide-coordinated analogue. Furthermore, a protein crystallographic study sheds light on the way the hydrolytic stability of the complexes is related to their interactions with HEWL.

RESULTS AND DISCUSSION

Synthesis and Characterization. Synthesis of the [RhCl(COD)(NHC)] complexes **8a−8c** was carried out based on examples of similar complexes reported by Monney et al.[17−19] and in analogy to a literature procedure for similar [IrCl(COD)(NHC)] complexes.[33] These methods required the preparation of pro-carbenes **2**, **5**, and **7**. Imidazolium salt **2** was obtained by nucleophilic substitution of 1-methylimidazole with methyl iodide.[30,31,33]

The His derivative **5** was synthesized from Boc-His(Trt)−OH (Scheme 1).[33] Final C-terminal deprotection provided the carboxylic acid **6** which was used for solid-phase peptide synthesis (SPPS) on HMBA resin to yield the imidazolium

https://dx.doi.org/10.1021/acs.inorgchem.0c02438
Inorg. Chem. XXXX, XXX, XXX−XXX

functionalized peptide **7** with an N-terminal Boc protection and a C-terminal methyl ester.[33,49]

Imidazolium salts **2**, **5**, and **7** were used for the synthesis of the desired rhodium complexes **8a**−**8c** by Ag_2O transmetalation according to Scheme 2, which was initially reported for the synthesis of [RhCl(COD)(NHC)] complexes[50] and was later adapted for [RhCl(COD)(NHC)] peptide conjugates[18,19] and iridium analogues.[33]

Scheme 2. Synthesis of the [RhCl(COD)(NHC)] Complexes 8a−8c by Ag_2O Transmetalation

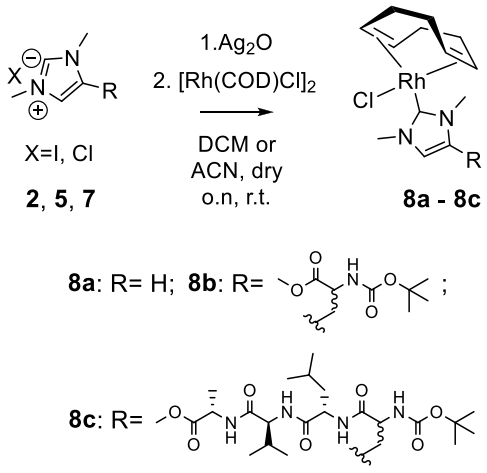

The ^{1}H nuclear magnetic resonance (NMR) spectra of the metal complexes showed the disappearance of the imidazolium proton found in the spectra of the pro-carbenes between 8.8 and 10.0 ppm. Additionally, the $^{13}C\{^1H\}$ NMR spectra of complexes **8a** and **8b** showed a significant low-field shift of the imidazolylidene carbon atom from around 137 ppm in **2** and **5** to 182−183 ppm after complexation.[50] Furthermore, these carbon atoms were detected as doublets, which can be assigned to the coupling of the rhodium center and the imidazolylidene carbon atom.[51] The coupling constants of 50.6 Hz for complex **8a** and 52.6 Hz for complex **8b** are in line with the values reported in the literature for [RhCl(COD)(NHC)] complexes.[51] The ^{1}H NMR spectrum of complex **8b** further revealed the formation of two rotamers present in a ratio of 1:0.7, an effect that has been described in detail for similar [RhCl(COD)(NHC)] complexes.[18,19,52] The effect was most obvious for the signal assigned to the C-terminal methyl group of the amino acid at 3.71−3.77 ppm, which resonates as a singlet in **5** but is clearly split into two distinct signals after complexation (Figure S1). The effect is less pronounced in the peptide complex **8c** but still visible. Together, these data provide unambiguous proof of the presence of a direct metal−carbon bond between the imidazolylidene carbon and the rhodium center of complexes **8a**−**8c**, which is particularly valuable for the peptide conjugate **8c** where several other functionalities on the peptide could potentially coordinate to the rhodium center. The purity of the peptide conjugate **8c** was shown by analytical high-pressure liquid chromatography (HPLC), where the peptide conjugate gave a significant shift in retention time after complexation in comparison to the free peptide, as also reported for similar [RhCl(COD)(NHC)] complexes (Figure S2).[52]

Assessment of Hydrolytic Stability by ^{1}H NMR Spectroscopy and HPLC. The hydrolytic stability of [RhCl(COD)(NHC)] complexes was previously analyzed by mass spectrometry.[23] The experiments revealed an initial chlorido/hydroxido ligand exchange followed by a subsequent substitution of the NHC ligand with solvent molecules.[23] These intermediates converted into halido-bridged dimers with the NHC ligand retained in some cases.[23] Similar [IrCl(COD)(NHC)] complexes have been reported to show time-dependent displacement of the COD ligand.[33] This process is assumed to produce a reactive intermediate capable of interacting with biomolecules.[29,31−33]

In order to follow up on these previous reports, the hydrolytic stability of **8a** was analyzed by time-dependent ^{1}H NMR spectroscopy. Thus, the rhodium complex **8a** was dissolved in deuterated acetonitrile, and ∼17% of water was added to the solution as previously reported for an analogous Ir complex.[33] Monitoring of the reaction during the next 48 h revealed two new peaks in the regions of 5.53 ppm (A, Figure 1) and 2.32 ppm (B, Figure 1). These were assigned to free COD, as found for the Ir congener of **8a**.[33] In order to confirm the observation, the experiment was repeated, and the sample was spiked after 48 h with COD, which resulted in the intensity of the peaks at 5.53 and 2.32 ppm to increase significantly (Figure S4). Complex **8c** was used as a small model system where a short biomolecule is directly included in the complex structure, and a similar experiment was conducted. Therein, the peptide complex showed the same behavior as its nonconjugated parent-compound **8a**, and new peaks were observed at 2.32 and 5.53 ppm that were equally assigned to free COD (Figure S3). Figure 2 shows a direct comparison of the hydrolytic behaviour of compounds **8a** and **8c**. Thus, COD displacement can be considered a main process in aqueous solution in addition to the previously reported chlorido exchange[23] that is not influenced by the nature of the NHC ligand.

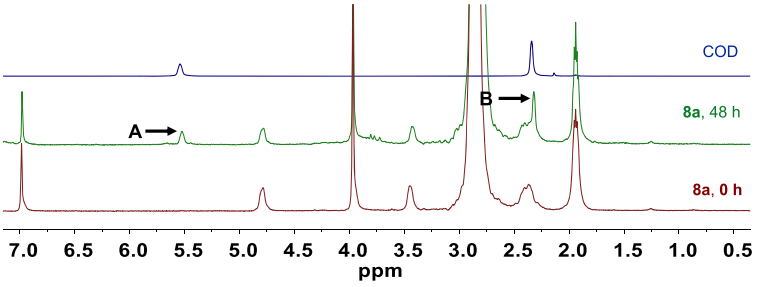

Figure 1. ^{1}H NMR spectra of complex **8a** after 0 h (lower trace) and 48 h (middle trace) in comparison to the spectrum of free COD (upper trace). The signals at around 5.53 and 2.32 ppm show a good overlap with the signals of free COD.

https://dx.doi.org/10.1021/acs.inorgchem.0c02438
Inorg. Chem. XXXX, XXX, XXX−XXX

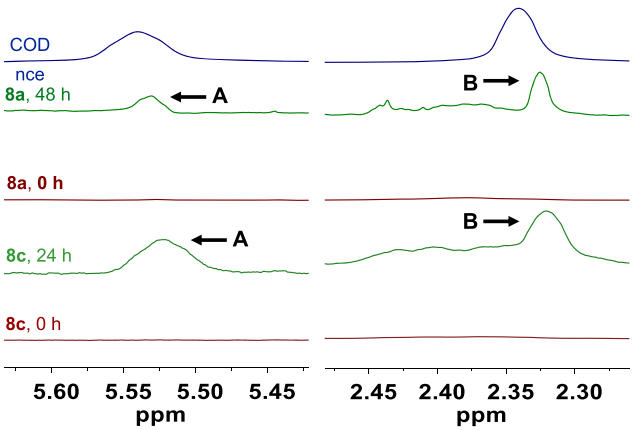

Figure 2. ^{1}H NMR spectra of complexes **8a** (middle traces) and **8c** (lower traces) after 0 and 48 h in comparison to the spectrum of COD (upper trace). The change in signals at around 5.53 (A) and 2.32 ppm (B) show a good overlay with the signals of COD.

In addition to the NMR investigations, complex **8c** was subjected to time-dependent analysis by analytical HPLC, which bears the possibility to isolate and characterize any potentially arising intermediates after COD release. For this purpose, **8c** was incubated at room temperature in a mixture of water and acetonitrile 1:1 (v/v), and samples were analyzed after defined time periods (see Figure S6). Minor changes in the chromatograms were observed over a period of 48 h. A small new peak B at a retention time of 8.1 min became however apparent. Characterization by ESI-mass spectrometry allowed to assign it to the free imidazolium-functionalized peptide which became detached from the complex. This was confirmed by a comparison of the retention time to that of the free peptide. This result is in line with the previously observed release of NHC ligands.[23] In contrast to the release of COD observed by the ^{1}H NMR spectroscopy within the first 24 h of incubation, NHC cleavage seems to be significantly slower and becomes apparent only after 48 h. These rather small changes observed for complex **8c** in the HPLC experiments and the significantly faster hydrolysis recorded in the NMR experiments may be due to the different experimental conditions in terms of water content (HPLC 50%, NMR 17%). Thus, we hypothesized that a higher water content may be beneficial for the stability of the complex. In order to assess this hypothesis with the model complex **8a**, its stability was characterized in deuterated phosphate buffered saline (PBS) with 10% of DMSO for solubility reasons. Indeed, in this biologically relevant buffer system, the ^{1}H NMR spectra of the sample measured after 24 and 48 h showed no significant changes and especially no COD release (see Figure S5). Acetonitrile is known for its ability to substitute ethylene and cyclooctene[53] as well as acetylacetonato[54] ligands in Rh(I)-NHC complexes. Thus, we conclude that the presence of high acetonitrile concentrations triggered the COD release in case of the NMR experiment, while complexes **8a** and **8c** have a high degree of stability in aqueous solutions including biologically relevant buffer systems.

Protein Interaction Studies by X-ray Crystallography. HEWL is a well-established model protein and has provided insightful data into the protein binding capabilities of metal-based complexes.[35,36,43,55,56] HEWL crystals were grown overnight in sodium chloride and sodium acetate at pH 4.7. The crystals were transferred to a solution of sodium nitrate and sodium acetate at pH 4.7 supplemented with **8b** (0.69 mg, 2 mg/mL) and soaked for 7 d and 4 weeks. Crystals were harvested after 7 d and 4 weeks and analyzed by X-ray diffraction at the MX1 beamline at the Australian Synchrotron. Both structures crystallized in the $P4_32_12$ space group, with the phases determined using molecular replacement with the search model 4NHI,[57] which located one molecule in the asymmetric unit. The sites of metalation were identified as peaks in an anomalous difference map based upon the anomalous diffraction of the Rh metal center.[58] The structures were refined to final R_{work}/R_{free} values of 0.19/0.22 at a resolution of 1.35 Å (7 days) and 0.20/0.25 at a resolution of 1.55 Å (4 weeks) (Supporting Information). When comparing the metalated structures to native HEWL (Protein Databank (PDB) ID 4NHI),[57] there were no major structural perturbations, with only localized changes to the positions of side chains (Supporting Information) occurred. This is shown in the small root-mean-square deviations (RMSD) of 0.241 Å after 7 days and slightly increased to 0.265 Å after 4 weeks.

The analysis of the crystal obtained after 7 d (PDB ID 6WRL) of soaking revealed a single anomalous peak at a peak height of 7.0σ, located near His15. The rhodium center was placed at the center of the anomalous density at a Rh−$N^{\epsilon 1}_{His15}$ bond length of 2.43 Å. The occupancy of the Rh center was set to 0.5 to match both the B-factors of the surrounding side chains, and the density level in both the $2F_o-F_c$ and F_o-F_c electron density maps (Figure 3 and Figure S7). Examination of refined $2F_o-F_c$ electron density maps revealed further density surrounding the metal center. However, the density could not be unambiguously assigned to structural components

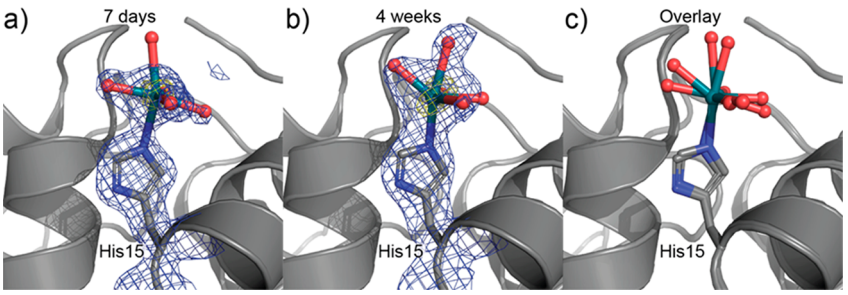

Figure 3. Details of the interaction between the Rh center and HEWL at site 1 with His15 coordinated to a rhodium center with an octahedral coordination sphere filled with five aqua/hydroxido ligands. The electron density ($2F_o-F_c$) maps are contoured at 1σ (blue maps), while the anomalous difference maps are contoured at 4σ (yellow maps). Adducts formed after (a) 7 days and (b) 4 weeks. (c) Overlay of the 7 day and 4 week interactions showing the similarity of the interactions.

https://dx.doi.org/10.1021/acs.inorgchem.0c02438
Inorg. Chem. XXXX, XXX, XXX−XXX

of compound **8b**, most likely due to the exchange of ligands as observed by NMR spectroscopy and HPLC. Therefore, we have assigned the density as aqua/hydroxido (OH_n; n = 1, 2) ligands at an average Rh−OH_n (n = 1, 2) bond distance of 2.35 Å (Figure 3a, Supporting Information). After 4 weeks of soaking, the interaction at the His15 site appears remarkably similar (Figure 3b, overlay shown in Figure 3c), with a peak height of 6.7σ and a Rh−$N^{\varepsilon 1}{}_{His15}$ bond distance of 2.20 Å, the occupancy (0.5) remained the same, and the average Rh−OH_n bond distance was similar to that previously observed (Figure 3b and Figure S8). These observations match the results from the stability studies and literature reports for the substitution of Cl, COD, and NHC ligands of organorhodium and -iridium compounds.[29−32] A similar type of adduct was observed when $RhCl_3$ was incubated with HEWL (PDB ID 3A94).[59]

An additional binding site was identified in the sample obtained after 4 weeks (PDB ID 6WRM) of incubation, which was located near Lys33 and was found with an anomalous peak height of 10.9σ. A second Rh center was placed at a Ru−$N^{\zeta 1}{}_{Lys33}$ bond distance of 2.28 Å. Similar to the binding site at His15, after refinement significant $2F_o-F_c$ density surrounding the metal center was observed (Supporting Information). The Rh center in *trans* position to $N^{\zeta 1}{}_{Lys33}$ appeared to be a crescent shaped density which suggested that the NHC remained bound (Supporting Information). The density is consistent with the imidazolylidene ligand being present but in multiple conformations, resulting in poorly defined electron density. To include the carbene ligand, two alternate conformations were modeled (Figure 4c and Figure S9).

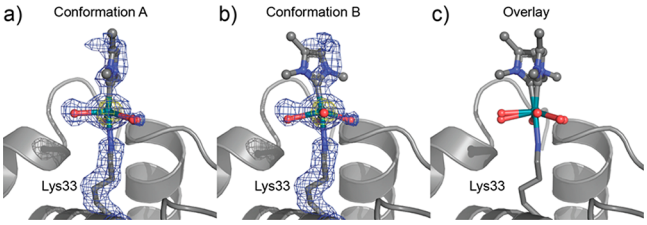

Figure 4. Details of the interaction at the second metalation site, which shows the Lys33 residue bound to rhodium with an octahedral coordination sphere featuring an imidazolylidene and four aqua ligands. The electron density maps are contoured at 1σ (blue maps), while the anomalous difference maps are contoured at 4σ (yellow maps). (a) Conformation A with an occupancy of 0.35. (b) Conformation B with an occupancy of 0.25. (c) Overlay of both conformations.

Cumulatively, the Rh center had an occupancy of 0.6, which was defined by the lack of negative density in the refined F_o-F_c map (Figure S10) and a comparison with the B-factor of surrounding side-chains. The alternative conformations A (Figure 4a) and B (Figure 4b), showed occupancies of 0.35 and 0.25, respectively, which gave both conformations similar B-factors (Supporting Information). The Rh−$C_{carbene}$ bond distance was 2.07 Å and is very similar to that found in Ru(NHC) complexes.[46,60] The ligands at the equatorial positions of the Rh center were identified as aqua or hydroxido (OH_n, n = 1, 2) ligands, however, they could not be unambiguously assigned. The NHC core was rotated by ∼67° about the C3 atom, whereby the C4 atoms of the alternate conformers are 1.73 Å away from each other. The OH_n ligands were also considered associated with a specific alternate conformation with average Rh−OH_n bond distances of 2.52 Å (conformation A) and 2.47 Å (conformation B). Confirmation of the interaction at Lys33 was made using phenix.polder (Figure S11) and simulated annealing composite omit maps (Figure S12). The positioning of Lys33 in the native non-adducted (4NHI) structure was compared to that with the adduct in the binding site (Figure S13). The binding to this site was much slower than occurred at His15. In the structure obtained for $RhCl_3$ with HEWL (3A94),[59] no interactions with an L-lysine residue were observed. Intriguingly, the reaction of **8b** with HEWL and substitution of the labile COD and chlorido ligands resulted in adducts of octahedral coordination geometry, while the prepared complexes are square planar Rh(I) compounds. This indicates oxidation of the Rh(I) center to Rh(III).

CONCLUSIONS

We report here the preparation of [RhCl(COD)(NHC)] complexes in which we varied the NHC ligand from a simple dimethyl derivative (**8a**) to a His-derived carbene (**8b**), and the latter was incorporated in a peptide backbone (**8c**). In an aqueous environment, two ligand exchange processes were observed. Analysis of the hydrolytic stability of **8a** and **8c** by time-dependent ^{1}H NMR spectroscopy revealed fast and pronounced COD release. However, when complex **8c** was analyzed by analytical HPLC, no significant COD release was detected. Instead, the complex showed slow a displacement of the NHC ligand, and small amounts of free peptide ligand were detected, a process that is significantly slower than the COD release observed in the NMR experiment. When considering the different experimental conditions, it was hypothesized that the water content (17% in case of the NMR experiment and 50% in case of the HPLC experiment) was the origin of the different decomposition processes. Indeed, when the stability of complex **8a** was assessed by ^{1}H NMR spectroscopy in deuterated PBS buffer, no COD release was observed. Thus, the overall outcome of these experiments suggests an excellent hydrolytic stability of both complexes **8a** and **8c** and further suggests that an external coordinating agent is necessary to trigger the COD release process. Both of these molecular processes, COD and NHC release, were considered when complex **8b** was investigated for its interaction with HEWL. The crystal structures obtained after 7 days and 4 weeks of soaking revealed adduct formation at His15, which is often observed for Rh[61−64] and other metal complexes,[35,41,43,46,65−74] while all the original ligands were substituted for aqua and/or hydroxido ligands. Over longer periods of incubation, a second adduct at Lys33 was observed with a rhodium fragment that still featured the NHC ligand, but all other ligands were exchanged by solvent molecules. This may demonstrate that the protein microenvironment acts as a trigger for the ligand exchange processes occurring at the Rh center similar to acetonitrile in the NMR experiment, resulting in release of COD and the chlorido ligand. Both interactions suggest a change from the initially square-planar structure to an octahedral geometry. This indicates oxidation of the metal center from Rh(I) to Rh(III), a feature which has been reported to occur in similar Ir(I) complexes upon peptide[33] and protein interaction,[29,31] the nature of the oxidant at this stage is unknown. However, while the present results clearly suggest that the oxidation either occurs upon or after protein interaction, the exact chronological order of the events remains the object of further studies. In conclusion, our investigations represent the first insight on the interaction of

https://dx.doi.org/10.1021/acs.inorgchem.0c02438
Inorg. Chem. XXXX, XXX, XXX−XXX

[RhCl(COD)(NHC)] and proteins at the molecular level and the related ligand exchange reactions occurring at the Rh center.

EXPERIMENTAL SECTION

Synthesis of Amino Acid Derivatives. Compounds **4**−**6** and peptide **7** were synthesized according to literature procedures.[33] The detailed description of the synthesis, solid-phase peptide synthesis, and the respective analytical data can be found in the Supporting Information.

Synthesis of [Rh(NHC)(COD)Cl] Complexes (8a−8c). *General Procedure.* In a heated Schlenk flask under N_2 atmosphere, 1 equiv of the respective imidazolium salt was dissolved in 15 mL of dry dichloromethane (DCM) (in case of ligands **2** and **5**) or dry acetonitrile (ACN) (in case of peptide **7**). The solution was degassed by three consecutive cycles of freeze−pump−thaw. After addition of 0.5 equiv of Ag_2O, the solution was left to stir at room temperature for 1 h in the dark, during which a disappearance of the black Ag_2O could be seen, followed by an addition of 0.5 equiv of $[Rh(COD)Cl]_2$ leading to a color change to bright yellow. The solution was then left to stir overnight at room temperature. Afterward the reaction mixture was filtered through Celite (DCM/MeOH 9:1), and the filtrate was concentrated under reduced pressure. Purification of the product was carried out by flash column chromatography (*n*-hexane/ethyl acetate 0:1 to 1:0), leading to the products as bright yellow solids. The peptide conjugate **8c** was further purified by semipreparative HPLC on a VarioPrep 125/10 Nucleodur C4 Gravity 5 μm column with a gradient of ACN/H_2O and 0.1% of trifluoroacetic acid (TFA) (5:95 to 95:5 v/v).

*Chloro-(1,5-cyclooctadiene)(1,3-dimethyl-1H-imidazol-3-ide)-rhodium(I) (**8a**).* Yield: 125 mg (0.33 mmol, 55%). Analytical data: ^{1}H NMR (200 MHz, chloroform-*d*) δ 6.79 (s, 2H, N−CH═CH−N), 5.01 (s, 2H, 2x COD CH), 4.06 (s, 6H, 2x N−CH_3), 3.28 (s, 2H, 2x COD CH), 2.39 (t, *J* = 7.1 Hz, 4H, 2x COD CH_2), 1.93 (m, 4H, 2x COD CH_2). ^{13}C NMR (101 MHz, chloroform-*d*) δ 182.7 (d, *J* = 50.6 Hz, N−C−N), 122.0 (N−CH═CH−N), 98.6 (d, *J* = 6.8 Hz, COD CH), 67.8 (d, *J* = 14.5 Hz, COD CH), 37.8 (N−CH_3), 33.1 (COD CH_2), 29.0 (COD CH_2), ESI-MS: *m*/*z* 307.5 $[M - Cl]^+$.

*Chloro-1,5-cyclooctadiene-[4-(2-((tert-butoxycarbonyl)amino)-3-methoxy-3-oxopropyl)-1,3-dimethyl-1H-imidazol-3-ide]-rhodium(I) (**8b**).* Yield: 60 mg (0.11 mmol, 39%). Analytical data: R_f (ehtylacetate/*n*-hexane, 1:1): 0.13. ^{1}H NMR (400 MHz, chloroform-*d*, mixture of two isomers) δ 6.60 (d, *J* = 15.7 Hz, 2H, 2x N−CH = C), 5.01 (m, 6H, 6x COD CH, NH), 4.55 (dd, *J* = 12.0, 7.6 Hz, 2H, 2x α-CH), 4.01 (m, 12H, 4x N−CH_3), 3.74 (d, *J* = 20.2 Hz, 6H, 2x O−CH_3), 3.27 (m, 4H, 2x COD CH), 2.93 (m, 4H, 2x β-CH_2), 2.39 (qd, *J* = 12.4, 10.0, 5.5 Hz, 8H, 4x COD CH_2), 1.94 (m, 8H, 4x COD CH_2), 1.42 (d, *J* = 19.7 Hz, 18H, 6x Boc CH_3). ^{13}C NMR (101 MHz, chloroform-*d*) δ 171.7 (COOMe), 155.1 (CO-NH), 129.1 (N−C═CH), 120.2 (N−CH═C), 98.6 (d, *J* = 10.1 Hz, COD CH), 80.5 (Boc quat. C), 68.0 (m, COD CH), 52.6 (m, COD CH, α-CH, O−CH_3), 37.8 (d, *J* = 8.0 Hz, N−CH_3), 35.1 (N−CH_3), 33.1 (m, COD CH_2), 31.7 (COD CH_2), 29.0 (m, COD CH_2), 28.4 (d, *J* = 6.5 Hz, Boc CH_3), 28.0 (d, *J* = 32.3 Hz, COD CH_2). ESI-MS: *m*/*z* 508.5 $[M - Cl]^+$, 565.9 $[M + Na]^+$.

*Chloro-1,5-cyclooctadiene-[5-(13-((tert-butoxycarbonyl)amino)-10-isobutyl-7-isopropyl-4-methyl-3,6,9,12-tetraoxo-2-oxa-5,8,11-triazatetradecan-14-yl)-1,3-dimethyl-1H-imidazol-3-ide]-rhodium-(I) (**8c**).* Yield: 13 mg (0.016 mmol, 32%). Analytical data: R_f (ethyl acetate): 0.50. ^{1}H NMR (300 MHz, chloroform-*d*, mixture of two isomers) δ 6.65 (s, 2H, 2x N−CH═C), 5.40 (m, 2H, 2x COD CH), 4.98 (s, 4H, 4x COD CH), 4.19 (m, 19H, 6x α-CH, 4x N−CH_3), 3.74 (d, *J* = 4.7 Hz, 6H, 2x O−CH_3), 3.48 (d, *J* = 3.1 Hz, 2H, 2x COD CH), 3.28 (s, 2H, 2x COD CH), 2.84 (m, 4H, 2x β-CH_2), 2.39 (d, *J* = 11.1 Hz, 8H, 4x COD CH_2), 2.01 (dd, *J* = 44.5, 8.7 Hz, 8H, 2x Val CH, 3x COD CH_2), 1.58 (q, *J* = 9.3, 8.9 Hz, 6H, 2x Leu CH, 2x Leu CH_2), 1.41 (t, *J* = 6.7 Hz, 24H, 6x Boc CH_3, 2x Ala CH_3), 0.93 (dq, *J* = 12.9, 5.6, 4.8 Hz, 24H, 4x Val CH_3, 4x Leu CH_3). ESI-MS: *m*/*z* 791.7 $[M - Cl]^+$. HR ESI-MS: *m*/*z* 791.3594 $[M - Cl]^+$, 849.3177 $[M + Na]^+$. Analytical HPLC retention time: (gradient: acetonitrile/H_2O 5:95 and 0.1% TFA to acetonitrile/H_2O 95:5 and 0.1% TFA, column: Macherey Nagel EC 125/4 Nucleodur C4 Gravity 5 μm): 8.6 min.

Protein Crystallography. HEWL crystals of 0.1−0.2 mm were grown from a reservoir solution consisting of sodium chloride (0.8 M) and sodium acetate (0.1 M, pH 4.7) which, in the crystallization drop, was mixed with an equal volume of HEWL (100 mg/mL).[75] Crystals formed within 24 h and were then transferred into a drop of reservoir solution of sodium nitrate (0.8 M) and sodium acetate (0.1 M, pH 4.7) supplemented with **8b** (0.69 mg, 2 mg/mL). The crystals were observed to turn orange after 3 d, and X-ray analysis was performed after soaking for periods of 1 week and 1 month. For this purpose, the soaked crystals were transferred into a cryoprotectant of 20% glycerol, sodium nitrate (0.8 M), and sodium acetate (0.1 M, pH 4.7) and flash frozen in liquid nitrogen.

Protein Crystal Data Collection and Analysis. X-ray diffraction data were collected on the crystallography beamline MX1 at the Australian Synchrotron.[76] Data were processed with XDS,[77] revealing that the protein crystallized in the space group $P4_32_12$. The structures were determined by molecular replacement using a monomer of lysozyme (PDB ID: 4NHI)[57] as a search model in PHASER.[78] The models were refined with iterative rounds of refinement and model building in REFMAC[79] and COOT.[80] Sodium ion placement was aided by the use of the WASP server at USF.[81] The $2F_o-F_c$, F_o-F_c, and anomalous difference maps were generated using FFT.[82] To further support the positioning of the organometallic moieties, maps were generated of unbiased density, of simulated annealing composite omit,[83] and with phenix.polder.[84] The compound fragment formed was reformatted (from the small molecule crystal structure of an analogous [Ir(Cl)(COD)(NHC)] complex)[85] using Gaussian,[86] and the final PDB and CIF files were generated by phenix.elbow.[87]

ASSOCIATED CONTENT

Supporting Information

The Supporting Information is available free of charge at https://pubs.acs.org/doi/10.1021/acs.inorgchem.0c02438.

General experimental information, detailed synthesis procedures for all compounds, supplementary figures and spectra (NMR, MS, including high-resolution MS of **8c**), chromatograms of all metal-containing compounds, and additional crystallographic data and figures (PDF)

AUTHOR INFORMATION

Corresponding Author

Nils Metzler-Nolte − *Inorganic Chemistry I − Bioinorganic Chemistry, Faculty of Chemistry and Biochemistry, Ruhr-Universität Bochum, 44801 Bochum, Germany;* orcid.org/0000-0001-8111-9959; Email: nils.metzler-nolte@rub.de

Authors

Isabelle M. Daubit − *Inorganic Chemistry I − Bioinorganic Chemistry, Faculty of Chemistry and Biochemistry, Ruhr-Universität Bochum, 44801 Bochum, Germany*

Matthew P. Sullivan − *School of Chemical Sciences and School of Biological Sciences, University of Auckland, Auckland 1142, New Zealand;* orcid.org/0000-0003-4181-4249

Milena John − *Inorganic Chemistry I − Bioinorganic Chemistry, Faculty of Chemistry and Biochemistry, Ruhr-Universität Bochum, 44801 Bochum, Germany*

David C. Goldstone − *School of Biological Sciences, University of Auckland, Auckland 1142, New Zealand;* orcid.org/0000-0003-0069-9408

Christian G. Hartinger − *School of Chemical Sciences, University of Auckland, Auckland 1142, New Zealand;* orcid.org/0000-0001-9806-0893

https://dx.doi.org/10.1021/acs.inorgchem.0c02438
Inorg. Chem. XXXX, XXX, XXX−XXX

Complete contact information is available at:
https://pubs.acs.org/10.1021/acs.inorgchem.0c02438

Author Contributions

#I.D. and M.S. contributed equally.

Notes

The authors declare no competing financial interest.

■ ACKNOWLEDGMENTS

We kindly acknowledge the work of Annika Krusenbaum and Marvin Heller who helped with the syntheses of His derivative **6** and rhodium complex **8b**. We are grateful to Martin Gartmann who helped record the NMR spectra of peptide complex **8c** and to Dr. Dirk Wolters for recording its high-resolution mass spectrum. This research was, in part, undertaken on the crystallography beamline MX1 at the Australian Synchrotron, Victoria, Australia with support from the NZ synchrotron group. M.P.S., D.C.G., and C.G.H. thank the University of Auckland (Frederick Douglas Brown Postgraduate Science Research Scholarship) and the Cancer Research Trust for financial support. Support to M.J. by Ruhr University Bochum through the LabExchange program during a lab placement in the Hartinger lab at the University of Auckland is gratefully acknowledged. N.M.-N. is grateful for a Julius-von-Haast Fellowship from the Royal Society of New Zealand.

■ REFERENCES

(1) Giraldi, T.; Zassinovich, G.; Mestroni, G. Antitumor action of planar organometallic rhodium(I) complexes. *Chem.-Biol. Interact.* **1974**, *9* (6), 389−394.
(2) Giraldi, T.; Sava, G.; Mestroni, G.; Zassinovich, G.; Stolfa, D. Antitumor action of iridium(I) and rhodium(I) complexes. *Chem.-Biol. Interact.* **1978**, *22* (2−3), 231−238.
(3) Noffke, A. L.; Habtemariam, A.; Pizarro, A. M.; Sadler, P. J. Designing organometallic compounds for catalysis and therapy. *Chem. Commun.* **2012**, *48* (43), 5219−5246.
(4) Leung, C.-H.; Zhong, H.-J.; Chan, D. S.-H.; Ma, D.-L. Bioactive iridium and rhodium complexes as therapeutic agents. *Coord. Chem. Rev.* **2013**, *257* (11−12), 1764−1776.
(5) Ma, D.-L.; Chan, D. S.-H.; Leung, C.-H. Group 9 Organometallic Compounds for Therapeutic and Bioanalytical Applications. *Acc. Chem. Res.* **2014**, *47* (12), 3614−3631.
(6) Soldevila-Barreda, J. J.; Habtemariam, A.; Romero-Canelón, I.; Sadler, P. J. Half-sandwich rhodium(III) transfer hydrogenation catalysts: Reduction of NAD+ and pyruvate, and antiproliferative activity. *J. Inorg. Biochem.* **2015**, *153*, 322−333.
(7) Soldevila-Barreda, J. J.; Sadler, P. J. Approaches to the design of catalytic metallodrugs. *Curr. Opin. Chem. Biol.* **2015**, *25*, 172−183.
(8) Ma, D.-L.; Wang, M.; Mao, Z.; Yang, C.; Ng, C.-T.; Leung, C.-H. Rhodium complexes as therapeutic agents. *Dalton Trans.* **2016**, *45* (7), 2762−2771.
(9) Truong, D.; Sullivan, M. P.; Tong, K. K. H.; Steel, T. R.; Prause, A.; Lovett, J. H.; Andersen, J. W.; Jamieson, S. M. F.; Harris, H. H.; Ott, I.; Weekley, C. M.; Hummitzsch, K.; Söhnel, T.; Hanif, M.; Metzler-Nolte, N.; Goldstone, D. C.; Hartinger, C. G. Potent Inhibition of Thioredoxin Reductase by the Rh Derivatives of Anticancer M(arene/Cp*)(NHC)Cl2 Complexes. *Inorg. Chem.* **2020**, *59* (5), 3281−9.
(10) Diéz-González, S.; Marion, N.; Nolan, S. P. N-Heterocyclic Carbenes in Late Transition Metal Catalysis. *Chem. Rev.* **2009**, *109*, 3612−3676.
(11) Korotkikh, N. I.; Saberov, V. S.; Glinyanaya, N. V.; Marichev, K. A.; Kiselyov, A. V.; Knishevitsky, A. V.; Rayenko, G. F.; Shvaika, O. P. Catalysis of Organic Reactions by Carbenes and Carbene Complexes. *Chem. Heterocycl. Compd.* **2013**, *49* (1), 19−38.
(12) Gichumbi, J. M.; Friedrich, H. B. Half-sandwich complexes of platinum group metals (Ir, Rh, Ru and Os) and some recent biological and catalytic applications. *J. Organomet. Chem.* **2018**, *866*, 123−143.
(13) Nelson, D. J.; Nolan, S. P. Quantifying and understanding the electronic properties of N-heterocyclic carbenes. *Chem. Soc. Rev.* **2013**, *42* (16), 6723−53.
(14) Nelson, D. J.; Nolan, S. P.; Falivene, L.; Poater, A.; Cavallo, L.; Wu, L.; Salvador, A.; Dorta, R.; Hoyos, M.; Guest, D.; Navarro, O.; Dierick, S.; Markó, I. E.; Wagers, P. O.; Shelton, K. L.; Panzner, M. J.; Tessier, C. A.; Youngs, W. J.; Lazreg, F.; Cazin, C. S. J.; Wurm, T.; Asiri, A. M.; Hashmi, A. S. K.; Poyatos, M.; Guisado-Barrios, G.; Peris, E.; Mavila, S.; Lemcoff, N. G.; Schwartsburd, L.; Whittlesey, M. K.; Haynes, M. T. I.; Jackson, E. P.; Montgomery, J.; Bellemin-Laponnaz, S.; Dagorne, S.; Murphy, L. J.; Robertson, K. N.; Masuda, J. D.; Clyburne, J. A. C.; Slaughter, L. M. *N-Heterocyclic Carbenes - Effective Tools for Organometallic Synthesis*; Wiley-VCH: Weinheim, 2014; p 543.
(15) Hopkinson, M. N.; Richter, C.; Schedler, M.; Glorius, F. An overview of N-heterocyclic carbenes. *Nature* **2014**, *510* (7506), 485−496.
(16) Sipos, G.; Dorta, R. Iridium complexes with monodentate N-heterocyclic carbene ligands. *Coord. Chem. Rev.* **2018**, *375*, 13−68.
(17) Monney, A.; Alberico, E.; Ortin, Y.; Muller-Bunz, H.; Gladiali, S.; Albrecht, M. Stereospecific synthesis and catalytic activity of L-histidylidene metal complexes. *Dalton Trans.* **2012**, *41* (29), 8813−8821.
(18) Monney, A.; Albrecht, M. A chelating tetrapeptide rhodium complex comprised of a histidylidene residue: biochemical tailoring of an NHC-Rh hydrosilylation catalyst. *Chem. Commun.* **2012**, *48* (89), 10960−10962.
(19) Monney, A.; Nastri, F.; Albrecht, M. Peptide-tethered monodentate and chelating histidylidene metal complexes: synthesis and application in catalytic hydrosilylation. *Dalton Trans.* **2013**, *42* (16), 5655−5660.
(20) McConnell, J. R.; Rananaware, D. P.; Ramsey, D. M.; Buys, K. N.; Cole, M. L.; McAlpine, S. R. A potential rhodium cancer therapy: Studies of a cytotoxic organorhodium(I) complex that binds DNA. *Bioorg. Med. Chem. Lett.* **2013**, *23* (9), 2527−2531.
(21) Simpson, P. V.; Schmidt, C.; Ott, I.; Bruhn, H.; Schatzschneider, U. Synthesis, Cellular Uptake and Biological Activity Against Pathogenic Microorganisms and Cancer Cells of Rhodium and Iridium N-Heterocyclic Carbene Complexes Bearing Charged Substituents. *Eur. J. Inorg. Chem.* **2013**, *2013* (32), 5547−5554.
(22) Oehninger, L.; Küster, L. N.; Schmidt, C.; Muñoz-Castro, A.; Prokop, A.; Ott, I. A Chemical-Biological Evaluation of Rhodium(I)-N-Heterocyclic Carbene Complexes as Prospective Anticancer Drugs. *Chem. - Eur. J.* **2013**, *19* (52), 17871−17880.
(23) Oehninger, L.; Spreckelmeyer, S.; Holenya, P.; Meier, S. M.; Can, S.; Alborzinia, H.; Schur, J.; Keppler, B. K.; Wölfl, S.; Ott, I. Rhodium(I) N-Heterocyclic Carbene Bioorganometallics as in Vitro Antiproliferative Agents with Distinct Effects on Cellular Signaling. *J. Med. Chem.* **2015**, *58* (24), 9591−9600.
(24) Zhang, J.-J.; Muenzner, J. K.; Abu el Maaty, M. A.; Karge, B.; Schobert, R.; Wölfl, S.; Ott, I. A multi-target caffeine derived rhodium(i) N-heterocyclic carbene complex: evaluation of the mechanism of action. *Dalton Trans.* **2016**, *45* (33), 13161−13168.
(25) Streciwilk, W.; Terenzi, A.; Misgeld, R.; Frias, C.; Jones, P. G.; Prokop, A.; Keppler, B. K.; Ott, I. Metal NHC Complexes with Naphthalimide Ligands as DNA-Interacting Antiproliferative Agents. *ChemMedChem* **2017**, *12* (3), 214−225.
(26) Streciwilk, W.; Terenzi, A.; Lo Nardo, F.; Prochnow, P.; Bandow, J. E.; Keppler, B. K.; Ott, I. Synthesis and Biological Evaluation of Organometallic Complexes Bearing Bis-1,8-naphthalimide Ligands. *Eur. J. Inorg. Chem.* **2018**, No. 26, 3104−3112.
(27) Streciwilk, W.; Terenzi, A.; Cheng, X.; Hager, L.; Dabiri, Y.; Prochnow, P.; Bandow, J. E.; Wölfl, S.; Keppler, B. K.; Ott, I. Fluorescent organometallic rhodium(I) and ruthenium(II) metallodrugs with 4-ethylthio-1,8-naphthalimide ligands: Antiproliferative

effects, cellular uptake and DNA-interaction. *Eur. J. Med. Chem.* **2018**, *156*, 148−161.
(28) Fan, R.; Bian, M.; Hu, L.; Liu, W. A new rhodium(I) NHC complex inhibits TrxR: In vitro cytotoxicity and in vivo hepatocellular carcinoma suppression. *Eur. J. Med. Chem.* **2019**, *183*, 111721−111736.
(29) Gothe, Y.; Marzo, T.; Messori, L.; Metzler-Nolte, N. Cytotoxic activity and protein binding through an unusual oxidative mechanism by an iridium(i)-NHC complex. *Chem. Commun.* **2015**, *51* (15), 3151−3153.
(30) Gothe, Y.; Marzo, T.; Messori, L.; Metzler-Nolte, N. Iridium(I) Compounds as Prospective Anticancer Agents: Solution Chemistry, Antiproliferative Profiles and Protein Interactions for a Series of Iridium(I) N-Heterocyclic Carbene Complexes. *Chem. - Eur. J.* **2016**, *22* (35), 12487−94.
(31) Gothe, Y. Iridium compounds as prospective anti-cancer agents: Biological investigations on novel iridium(I)-NHC complexes. *Ph.D. Thesis*, Ruhr-Universität Bochum, Bochum, 2016.
(32) Gothe, Y.; Romero-Canelón, I.; Marzo, T.; Sadler, P. J.; Messori, L.; Metzler-Nolte, N. Synthesis and Mode of Action Studies on Iridium(I)-NHC Anticancer Drug Candidates. *Eur. J. Inorg. Chem.* **2018**, *2018* (20−21), 2461−2470.
(33) Daubit, I. M.; Metzler-Nolte, N. On the interaction of N-heterocyclic carbene Ir+I complexes with His and Cys containing peptides. *Dalton Trans.* **2019**, *48* (36), 13662−13673.
(34) Ferraro, G.; Gabbiani, C.; Merlino, A. First Crystal Structure for a Gold Carbene-Protein Adduct. *Bioconjugate Chem.* **2016**, *27* (7), 1584−7.
(35) McNae, I. W.; Fishburne, K.; Habtemariam, A.; Hunter, T. M.; Melchart, M.; Wang, F.; Walkinshaw, M. D.; Sadler, P. J. Half-sandwich arene ruthenium(II)-enzyme complex. *Chem. Commun.* **2004**, No. 16, 1786−7.
(36) Casini, A.; Mastrobuoni, G.; Temperini, C.; Gabbiani, C.; Francese, S.; Moneti, G.; Supuran, C. T.; Scozzafava, A.; Messori, L. ESI mass spectrometry and X-ray diffraction studies of adducts between anticancer platinum drugs and hen egg white lysozyme. *Chem. Commun.* **2007**, No. 2, 156−8.
(37) Zobi, F.; Spingler, B. Post-Protein-Binding Reactivity and Modifications of the fac-[Re(CO)3]+ Core. *Inorg. Chem.* **2012**, *51* (3), 1210−1212.
(38) Pinato, O.; Musetti, C.; Farrell, N. P.; Sissi, C. Platinum-based drugs and proteins: Reactivity and relevance to DNA adduct formation. *J. Inorg. Biochem.* **2013**, *122*, 27−37.
(39) Muegge, C.; Marzo, T.; Massai, L.; Hildebrandt, J.; Ferraro, G.; Rivera-Fuentes, P.; Metzler-Nolte, N.; Merlino, A.; Messori, L.; Weigand, W. Platinum(II) Complexes with O,S Bidentate Ligands: Biophysical Characterization, Antiproliferative Activity, and Crystallographic Evidence of Protein Binding. *Inorg. Chem.* **2015**, *54* (17), 8560−8570.
(40) Hanif, M.; Moon, S.; Sullivan, M. P.; Movassaghi, S.; Kubanik, M.; Goldstone, D. C.; Sohnel, T.; Jamieson, S. M. F.; Hartinger, C. G. Anticancer activity of Ru- and Os(arene) compounds of a maleimide-functionalized bioactive pyridinecarbothioamide ligand. *J. Inorg. Biochem.* **2016**, *165*, 100−7.
(41) Ferraro, G.; Pica, A.; Russo Krauss, I.; Pane, F.; Amoresano, A.; Merlino, A. Effect of temperature on the interaction of cisplatin with the model protein hen egg white lysozyme. *JBIC, J. Biol. Inorg. Chem.* **2016**, *21* (4), 433−442.
(42) Messori, L.; Merlino, A. Cisplatin binding to proteins: A structural perspective. *Coord. Chem. Rev.* **2016**, *315*, 67−89.
(43) Sullivan, M. P.; Groessl, M.; Meier, S. M.; Kingston, R. L.; Goldstone, D. C.; Hartinger, C. G. The metalation of hen egg white lysozyme impacts protein stability as shown by ion mobility mass spectrometry, differential scanning calorimetry, and X-ray crystallography. *Chem. Commun.* **2017**, *53* (30), 4246−4249.
(44) Casini, A.; Gabbiani, C.; Sorrentino, F.; Rigobello, M. P.; Bindoli, A.; Geldbach, T. J.; Marrone, A.; Re, N.; Hartinger, C. G.; Dyson, P. J.; Messori, L. Emerging protein targets for anticancer metallodrugs: inhibition of thioredoxin reductase and cathepsin B by antitumor ruthenium(II)-arene compounds. *J. Med. Chem.* **2008**, *51* (21), 6773−81.
(45) Oehninger, L.; Stefanopoulou, M.; Alborzinia, H.; Schur, J.; Ludewig, S.; Namikawa, K.; Munoz-Castro, A.; Koster, R. W.; Baumann, K.; Wolfl, S.; Sheldrick, W. S.; Ott, I. Evaluation of arene ruthenium(II) N-heterocyclic carbene complexes as organometallics interacting with thiol and selenol containing biomolecules. *Dalton Trans.* **2013**, *42* (5), 1657−66.
(46) Sullivan, M. P.; Nieuwoudt, M. K.; Bowmaker, G. A.; Lam, N. Y. S.; Truong, D.; Goldstone, D. C.; Hartinger, C. G. Unexpected arene ligand exchange results in the oxidation of an organoruthenium anticancer agent: the first X-ray structure of a protein-Ru(carbene) adduct. *Chem. Commun.* **2018**, *54* (48), 6120−6123.
(47) Ferraro, G.; Marzo, T.; Infrasca, T.; Cilibrizzi, A.; Vilar, R.; Messori, L.; Merlino, A. A case of extensive protein platination: the reaction of lysozyme with a Pt(ii)-terpyridine complex. *Dalton Trans.* **2018**, *47* (26), 8716−8723.
(48) Helliwell, J.; Tanley, S.; Schreurs, A.; Kroon-Batenburg, L. M. J., Cisplatin coordination chemistry determination at hen egg white lysozyme His15 with ligand distances and angles, and their standard uncertainties, and also reporting a split occupancy effect. arXiv (Biomolecules), June 4, 2016, 1606.01372, ver. 1. https://arxiv.org/abs/1606.01372, accessed November 5, 2020.
(49) Abd-Elgaliel, W. R.; Gallazzi, F.; Lever, S. Z. Total solid-phase synthesis of bombesin analogs with different functional groups at the C-terminus. *J. Pept. Sci.* **2007**, *13* (7), 487−492.
(50) Chianese, A. R.; Li, X.; Janzen, M. C.; Faller, J. W.; Crabtree, R. H. Rhodium and Iridium Complexes of N-Heterocyclic Carbenes via Transmetalation: Structure and Dynamics. *Organometallics* **2003**, *22* (8), 1663−1667.
(51) Frey, G. D.; Herdtweck, E.; Herrmann, W. A. Structural investigations of metalcarbonyl complexes with acyclic diamino carbenes. *J. Organomet. Chem.* **2006**, *691* (11), 2465−2478.
(52) Daubit, I. M.; Wolf, J.; Metzler-Nolte, N. Rhodium(I) and Iridium(I) N-Heterocyclic carbene complexes of imidazolium functionalized amino acids and peptides. *J. Organomet. Chem.* **2020**, *909*, 121096.
(53) Palacios, L.; Di Giuseppe, A.; Castarlenas, R.; Lahoz, F. J.; Pérez-Torrente, J. J.; Oro, L. A. Pyridine versus acetonitrile coordination in rhodium-N-heterocyclic carbene square-planar complexes. *Dalton Trans.* **2015**, *44* (12), 5777−5789.
(54) Palacios, L.; Di Giuseppe, A.; Opalinska, A.; Castarlenas, R.; Pérez-Torrente, J. J.; Lahoz, F. J.; Oro, L. A. Labile Rhodium(I)-N-Heterocyclic Carbene Complexes. *Organometallics* **2013**, *32* (9), 2768−2774.
(55) Messori, L.; Marzo, T.; Merlino, A. The X-ray structure of the complex formed in the reaction between oxaliplatin and lysozyme. *Chem. Commun.* **2014**, *50* (61), 8360−8362.
(56) Messori, L.; Merlino, A. Ruthenium metalation of proteins: the X-ray structure of the complex formed between NAMI-A and hen egg white lysozyme. *Dalton Trans.* **2014**, *43* (16), 6128−31.
(57) Lim, H.; Rho, J.; Hyun, J. K.; Kim, Y. J. Crystal structure of Hen egg-white lysozyme in Tris buffer at pH 7.5 with Magnesium formate. *RCSB Protein Databank*, 2014. https://www.rcsb.org/structure/4NHI, accessed November 5, 2020.
(58) Strahs, G.; Kraut, J. Low-resolution electron-density and anomalous-scattering-density maps of Chromatium high-potential iron protein. *J. Mol. Biol.* **1968**, *35* (3), 503−512.
(59) Ueno, T.; Abe, S.; Koshiyama, T.; Ohki, T.; Hikage, T.; Watanabe, Y. Elucidation of Metal-Ion Accumulation Induced by Hydrogen Bonds on Protein Surfaces by Using Porous Lysozyme Crystals Containing Rh(III) Ions as the Model Surfaces. *Chem. - Eur. J.* **2010**, *16* (9), 2730−2740.
(60) Hollering, M.; Albrecht, M.; Kühn, F. E. Bonding and Catalytic Application of Ruthenium N-Heterocyclic Carbene Complexes Featuring Triazole, Triazolylidene, and Imidazolylidene Ligands. *Organometallics* **2016**, *35* (17), 2980−2986.
(61) Satake, Y.; Abe, S.; Okazaki, S.; Ban, N.; Hikage, T.; Ueno, T.; Nakajima, H.; Suzuki, A.; Yamane, T.; Nishiyama, H.; Watanabe, Y.

https://dx.doi.org/10.1021/acs.inorgchem.0c02438
Inorg. Chem. XXXX, XXX, XXX−XXX

Incorporation of a Phebox Rhodium Complex into apo-Myoglobin Affords a Stable Organometallic Protein Showing Unprecedented Arrangement of the Complex in the Cavity. *Organometallics* **2007**, *26* (20), 4904−4908.
(62) Abe, S.; Hirata, K.; Ueno, T.; Morino, K.; Shimizu, N.; Yamamoto, M.; Takata, M.; Yashima, E.; Watanabe, Y. Polymerization of Phenylacetylene by Rhodium Complexes within a Discrete Space of apo-Ferritin. *J. Am. Chem. Soc.* **2009**, *131* (20), 6958−6960.
(63) Zimbron, J. M.; Heinisch, T.; Schmid, M.; Hamels, D.; Nogueira, E. S.; Schirmer, T.; Ward, T. R. A Dual Anchoring Strategy for the Localization and Activation of Artificial Metalloenzymes Based on the Biotin-Streptavidin Technology. *J. Am. Chem. Soc.* **2013**, *135* (14), 5384−5388.
(64) Ferraro, G.; Pratesi, A.; Messori, L.; Merlino, A. Protein interactions of dirhodium tetraacetate: a structural study. *Dalton Trans.* **2020**, *49* (8), 2412−2416.
(65) Casini, A.; Mastrobuoni, G.; Temperini, C.; Gabbiani, C.; Francese, S.; Moneti, G.; Supuran, C. T.; Scozzafava, A.; Messori, L. ESI mass spectrometry and X-ray diffraction studies of adducts between anticancer platinum drugs and hen egg white lysozyme. *Chem. Commun.* **2007**, No. 2, 156−158.
(66) Santos-Silva, T.; Mukhopadhyay, A.; Seixas, J. D.; Bernardes, G. J. L.; Romão, C. C.; Romão, M. J. CORM-3 Reactivity toward Proteins: The Crystal Structure of a Ru(II) Dicarbonyl-Lysozyme Complex. *J. Am. Chem. Soc.* **2011**, *133* (5), 1192−1195.
(67) Tanley, S.; Schreurs, A.; Kroon-Batenburg, L. M. J.; Helliwell, J. Room-temperature X-ray diffraction studies of cisplatin and carboplatin binding to His15 of HEWL after prolonged chemical exposure. *Acta Crystallogr., Sect. F: Struct. Biol. Cryst. Commun.* **2012**, *F68*, 1300−6.
(68) Vergara, A.; D'Errico, G.; Montesarchio, D.; Mangiapia, G.; Paduano, L.; Merlino, A. Interaction of Anticancer Ruthenium Compounds with Proteins: High-Resolution X-ray Structures and Raman Microscopy Studies of the Adduct between Hen Egg White Lysozyme and AziRu. *Inorg. Chem.* **2013**, *52* (8), 4157−4159.
(69) Messori, L.; Marzo, T.; Gabbiani, C.; Valdes, A. A.; Quiroga, A. G.; Merlino, A. Peculiar Features in the Crystal Structure of the Adduct Formed between cis-PtI2(NH3)2 and Hen Egg White Lysozyme. *Inorg. Chem.* **2013**, *52* (24), 13827−13829.
(70) Tanley, S. W. M.; Helliwell, J. R. Structural dynamics of cisplatin binding to histidine in a protein. *Struct. Dyn.* **2014**, *1* (3), 034701.
(71) Tabe, H.; Fujita, K.; Abe, S.; Tsujimoto, M.; Kuchimaru, T.; Kizaka-Kondoh, S.; Takano, M.; Kitagawa, S.; Ueno, T. Preparation of a Cross-Linked Porous Protein Crystal Containing Ru Carbonyl Complexes as a CO-Releasing Extracellular Scaffold. *Inorg. Chem.* **2015**, *54* (1), 215−220.
(72) Seixas, J. D.; Santos, M. F. A.; Mukhopadhyay, A.; Coelho, A. C.; Reis, P. M.; Veiros, L. F.; Marques, A. R.; Penacho, N.; Gonçalves, A. M. L.; Romão, M. J.; Bernardes, G. J. L.; Santos-Silva, T.; Romão, C. C. A contribution to the rational design of Ru(CO)3Cl2L complexes for in vivo delivery of CO. *Dalton Trans.* **2015**, *44* (11), 5058−5075.
(73) Pontillo, N.; Ferraro, G.; Messori, L.; Tamasi, G.; Merlino, A. Ru-Based CO releasing molecules with azole ligands: interaction with proteins and the CO release mechanism disclosed by X-ray crystallography. *Dalton Trans.* **2017**, *46* (29), 9621−9629.
(74) Tamasi, G.; Merlino, A.; Scaletti, F.; Heffeter, P.; Legin, A. A.; Jakupec, M. A.; Berger, W.; Messori, L.; Keppler, B. K.; Cini, R. {Ru(CO)x}-Core complexes with benzimidazole ligands: synthesis, X-ray structure and evaluation of anticancer activity in vivo. *Dalton Trans.* **2017**, *46* (9), 3025−3040.
(75) Blake, C. C. F.; Fenn, R. H.; Johnson, L. N.; Koenig, D. F.; Mair, G. A.; North, A. C. T.; Oldham, J. W. H.; Phillips, D. C.; Poljak, R. J.; Sarma, V. R.; Vernon, C. A. How the structure of lysozyme was actually determined. In *International Tables for Crystallography*; Rossmann, M. G.; Arnold, E., Eds.; International Union of Crystallography: Chester, England, 2006; Vol. *F*.
(76) Cowieson, N. P.; Aragao, D.; Clift, M.; Ericsson, D. J.; Gee, C.; Harrop, S. J.; Mudie, N.; Panjikar, S.; Price, J. R.; Riboldi-Tunnicliffe, A.; Williamson, R.; Caradoc-Davies, T. MX1: a bending-magnet crystallography beamline serving both chemical and macromolecular crystallography communities at the Australian Synchrotron. *J. Synchrotron Radiat.* **2015**, *22* (1), 187−90.
(77) Kabsch, W. Integration, scaling, space-group assignment, and post-refinement. *Acta Crystallogr., Sect. D: Biol. Crystallogr.* **2010**, *66*, 133−144.
(78) McCoy, A. J.; Grosse-Kunstleve, R. W.; Adams, P. D.; Winn, M. D.; Storoni, L. C.; Read, R. J. Phaser crystallographic software. *J. Appl. Crystallogr.* **2007**, *40*, 658−674.
(79) Murshudov, G. N.; Vagin, A. A.; Dodson, E. J. Refinement of Macromolecular Structures by the Maximum-Likelihood Method. *Acta Crystallogr., Sect. D: Biol. Crystallogr.* **1997**, *53* (3), 240−255.
(80) Emsley, P.; Cowtan, K. Coot: model-building tools for molecular graphics. *Acta Crystallogr., Sect. D: Biol. Crystallogr.* **2004**, *60*, 2126−2132.
(81) Nayal, M.; Di Cera, E. Valence screening of water in protein crystals reveals potential Na+ binding sites. *J. Mol. Biol.* **1996**, *256* (2), 228−234.
(82) Read, R. J.; Schierbeek, A. J. A phased translation function. *J. Appl. Crystallogr.* **1988**, *21* (5), 490−495.
(83) Terwilliger, T. C.; Grosse-Kunstleve, R. W.; Afonine, P. V.; Moriarty, N. W.; Adams, P. D.; Read, R. J.; Zwart, P. H.; Hung, L. W. Iterative-build OMIT maps: map improvement by iterative model building and refinement without model bias. *Acta Crystallogr., Sect. D: Biol. Crystallogr.* **2008**, *64*, 515−524.
(84) Liebschner, D.; Afonine, P. V.; Moriarty, N. W.; Poon, B. K.; Sobolev, O. V.; Terwilliger, T. C.; Adams, P. D. Polder maps: improving OMIT maps by excluding bulk solvent. *Acta Crystallogr., Sect. D: Biol. Crystallogr.* **2017**, *73* (2), 148−57.
(85) Daubit, I. M. Peptide-Conjugation and Luminescence Cell Imaging of Cytotoxic Iridium and Rhodium N-Heterocyclic Carbene Complexes. *Ph.D. Thesis*, Ruhr University Bochum, Bochum, 2020.
(86) Frisch, M. J.; Trucks, G. W.; Schlegel, H. B.; Scuseria, G. E.; Robb, M. A.; Cheeseman, J. R.; Scalmani, G.; Barone, V.; Mennucci, B.; Petersson, G. A.; Nakatsuji, H.; Caricato, M.; Li, X.; Hratchian, H. P.; Izmaylov, A. F.; Bloino, J.; Zheng, G.; Sonnenberg, J. L.; Hada, M.; Ehara, M.; Toyota, K.; Fukuda, R.; Hasegawa, J.; Ishida, M.; Nakajima, T.; Honda, Y.; Kitao, O.; Nakai, H.; Vreven, T.; Montgomery, J. A.; Peralta, J. E.; Ogliaro, F.; Bearpark, M.; Heyd, J. J.; Brothers, E.; Kudin, K. N.; Staroverov, V. N.; Kobayashi, R.; Normand, J.; Raghavachari, K.; Rendell, A.; Burant, J. C.; Iyengar, S. S.; Tomasi, J.; Cossi, M.; Rega, N.; Millam, J. M.; Klene, M.; Knox, J. E.; Cross, J. B.; Bakken, V.; Adamo, C.; Jaramillo, J.; Gomperts, R.; Stratmann, R. E.; Yazyev, O.; Austin, A. J.; Cammi, R.; Pomelli, C.; Ochterski, J. W.; Martin, R. L.; Morokuma, K.; Zakrzewski, V. G.; Voth, G. A.; Salvador, P.; Dannenberg, J. J.; Dapprich, S.; Daniels, A. D.; Farkas Foresman, J. B.; Ortiz, J. V.; Cioslowski, J.; Fox, D. J. *Gaussian 09*, Revision B.01; Gaussian, Inc.: Wallingford CT, 2009.
(87) Moriarty, N. W.; Grosse-Kunstleve, R. W.; Adams, P. D. electronic Ligand Builder and Optimization Workbench (eLBOW): a tool for ligand coordinate and restraint generation. *Acta Crystallogr., Sect. D: Biol. Crystallogr.* **2009**, *65*, 1074−1080.

https://dx.doi.org/10.1021/acs.inorgchem.0c02438
Inorg. Chem. XXXX, XXX, XXX−XXX